



HAL
open science

On the interest of ambipolar materials for gas sensing

Amélie Wannebroucq, Seydou Ouédraogo, Rita Meunier-Prest, Jean-Moïse Suisse, Mabinty Bayo, Marcel Bouvet

► To cite this version:

Amélie Wannebroucq, Seydou Ouédraogo, Rita Meunier-Prest, Jean-Moïse Suisse, Mabinty Bayo, et al.. On the interest of ambipolar materials for gas sensing. *Sensors and Actuators B: Chemical*, 2018, 258, pp.657-664. 10.1016/j.snb.2017.11.146 . hal-02295846

HAL Id: hal-02295846

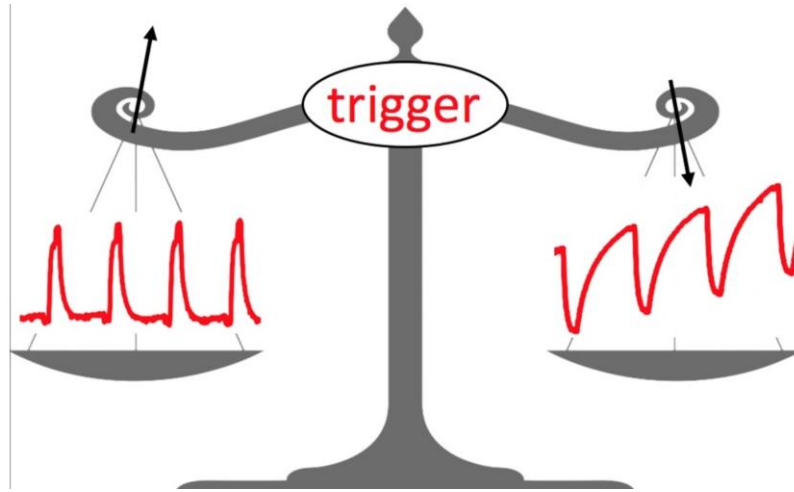
<https://hal.science/hal-02295846>

Submitted on 24 Sep 2019

HAL is a multi-disciplinary open access archive for the deposit and dissemination of scientific research documents, whether they are published or not. The documents may come from teaching and research institutions in France or abroad, or from public or private research centers.

L'archive ouverte pluridisciplinaire **HAL**, est destinée au dépôt et à la diffusion de documents scientifiques de niveau recherche, publiés ou non, émanant des établissements d'enseignement et de recherche français ou étrangers, des laboratoires publics ou privés.

Graphical abstract



Highlights

- Ambipolar materials exhibit a unique feature in chemosensing.
- Humidity can act as a trigger between p and n-type behaviors.
- The tuning of the electronic properties of sensing materials is of importance.

On the interest of ambipolar materials for gas sensing

Amélie Wannebroucq^a, Seydou Ouedraogo^b, Rita Meunier-Prest^a, Jean-Moïse Suisse^a, Mabinty Bayo^b, Marcel Bouvet^{a*}

^a*Institut de Chimie Moléculaire de l'Université de Bourgogne (ICMUB), UMR CNRS 6302, Univ. Bourgogne Franche-Comté, 9 avenue Alain Savary, 21078 Dijon cedex, France. Fax: +33-380-396-098; Tel: +33-380-396-086; E-mail: marcel.bouvet@u-bourgogne.fr*

^b*Laboratoire de Chimie Moléculaire et de Matériaux, Université de Ouagadougou, 03 BP 7021, Ouagadougou, Burkina Faso*

Abstract

Based on the electrochemical properties of a series of metallophthalocyanines this article shows that the phthalocyanine bearing four alkoxy groups and twelve fluorine atoms behaves approximately as those with eight fluorine atoms. This indicates that the electron-donating effect of one alkoxy group balances the electro-withdrawing effect of one fluorine atom. We engaged three metallophthalocyanines, namely the octafluoro copper phthalocyanine, Cu(F₈Pc), an octaester metallophthalocyanine and a phthalocyanine bearing four alkoxy groups and twelve fluorine atoms, Zn(T₄F₁₂Pc), in building original conductometric transducers that are Molecular Semiconductor - Doped Insulator heterojunctions (MSDIs) in association with the highly conductive lutetium bisphthalocyanine, LuPc₂. Whereas the octaester derivative and Zn(T₄F₁₂Pc) exhibited a negative response to ammonia, as expected for p-type materials, Cu(F₈Pc) exhibited a particular behavior. At low humidity levels, 30 and 10 % rh, the current of the Cu(F₈Pc)/LuPc₂ MSDI decreases, similarly to p-type devices, but at higher relative humidity values, 70 % rh, the current increases under ammonia, which is the signature of a n-type behavior. This ambipolar behavior is unique amongst semiconducting sensing materials. This work opens the way to the study of ambipolar materials as sensing materials for the development of a new type of conductometric gas sensors.

1. Introduction

Most molecular materials used in organic electronics only exhibit an unipolar behavior, with either electrons or holes as majority charge carriers [1,2]. However, devices that can transport both electrons and holes are very important to design complementary integrated circuits without requiring the implementation of two types of field-effect transistors with p- or n-type channels. The first ambipolar behavior ever observed in an OFET was with the lutetium bisphthalocyanine, LuPc₂, as molecular semiconductor [3]. Although the term ambipolar was not used in the published paper, the authors did observe both n and p channels, under vacuum and in air, respectively. This clearly indicates that the density of charge carriers of both p- and n-type can be high in LuPc₂, depending on the experimental conditions. This is a consequence of its particularly low energy gap, ca. 0.5 eV [4,5], resulting from its radical nature. Moreover, in this case, the SiO₂ dielectric material was modified by long alkyl chains, known for avoiding charge trapping at the semiconductor – dielectric material interface [5].

Generally, ambipolar devices result from the combination of two materials, including blends of polymers. There are several examples in the literature, including poly-phenylene vinylene or polyhexylthiophene as hole-transporting material with a fullerene derivative (PCBM) as electron-transporting semiconductor [6], a pentacene derivative associated with a perylenediimide [7] or a perfluorophthalocyanine [8] as n-type materials, blends of benzimidazolebenzophenanthroline ladder polymer (BBL) and copper phthalocyanine [9], and blends of two phthalocyanines, one bearing octyloxycarbonyl substituents, Cu((COOC₈H₁₇)₈Pc), and the other one alkoxy chains, Cu((OC₈H₁₇)₈Pc) [10]. Organic heterostructures, including p-n heterojunctions and ambipolar transistors, have been described in detail by H. Wang and D. Yan [13]. We can also cite interesting reviews on ambipolar OFETs, by H. Sirringhaus [1,2,11,12].

The historical LuPc₂ example aside, several families of molecules were reported that exhibit an ambipolar behavior with a single semiconductor layer capable of conducting both electrons and holes. For instance, the [6,6]-phenyl-C61-butyric acid methyl ester (PCBM) – a C60 derivative that is known as a n-type material can exhibit a p-type channel with gold electrodes on SiO₂ treated with hexamethyldisilazane as the dielectric material [14]. In the same way, a donor–acceptor conjugated polymer derived from BDOPV (benzodifurandione-

based oligo p-phenylene vinylene) exhibited a n-type behavior under vacuum and an ambipolar behavior when doped by oxygen [15].

From these examples, it is clear that particular operating conditions of the devices and specific atmospheres are required to observe an ambipolar charge transport. Donor–acceptor copolymers based on naphthalenediimide acceptor and (E)-2-(2-(thiophen-2-yl)vinyl)thiophene donor [16], or on polyfluorene derivatives [6], which have a band gap energy of 1.55 eV, are also nice examples of single component ambipolar materials. There is also the work of Y. Chen on lanthanide double decker [17] and triple decker complexes [18,19]. These cases are similar to the abovementioned LuPc₂ complex, since the ambipolarity results from the low energy gap, ca. 0.5 and 1.0 eV for lanthanide double and triple decker complexes, respectively. In addition, halogenated tetracene and pentacene and heteroatoms containing acenes [20-22], quinoidal quaterthiophen derivatives and tetracyanothienoquinoids [23,24] can also lead to an ambipolar behavior.

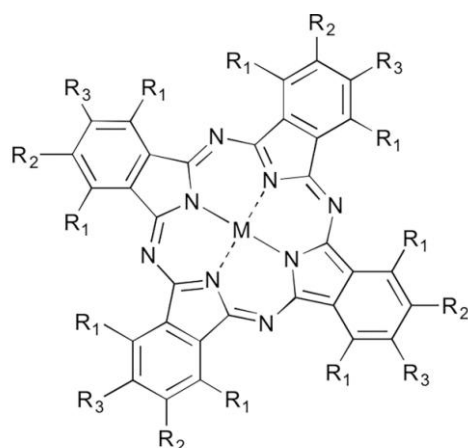
The ambipolar character of a material can be anticipated from the knowledge of the energy of its frontier orbitals, HOMOs and LUMOs [25], but relatively to the work function of the electrodes, since it determines whether charge injection is likely [2]. However, the emergence of such a behavior and its observation is highly dependent on the morphology of materials [9]. Tuning of electronic properties of materials can be achieved by the introduction of electron-donating or electron-withdrawing substituents on macrocyclic molecules [26-28]. It is well-known that fluorine substituted macrocycles exhibit stabilized frontier orbitals compared to non substituted counterparts, e.g. by 1.2 eV for hexadecafluoro-metallophthalocyanines, M(F₁₆Pc), relatively to the non fluorinated phthalocyanines, MPc [29]. Thus, perfluorinated phthalocyanines are n-type materials whereas non substituted phthalocyanines are p-type materials. The introduction of fluorine atoms on the phthalocyanine ring leads to n-type semiconductors useful to get n-type OFETs [30] and p-n heterojunctions [31], which can be used as gas sensors [32]. It is worth mentioning that the effect of the central metal of metallophthalocyanines on their chemosensing properties is rather weak compared to the electronic effect of substituents on the macrocycle. However, A. C. Kummel and W. C. Trogler reported the effect of the coordination strength of analytes on the central metal for five metallophthalocyanine resistors studied towards a series of VOCs [33].

Reported examples of ambipolar devices used for chemosensing are very rare. Thus, an

ambipolar hybrid organic-inorganic thin film transistor, containing pentacene and zinc oxide as semiconductors, was employed as an ethanol vapor sensor [34]. In p-channel accumulation mode, a decrease of current with the introduction of analyte was observed, while in the n-channel triode mode, an increase in current with analyte delivery was observed. In this case, the ambipolarity allowed for carrying out chemosensing experiments in two different operation modes. Another example is the one combining n and p phthalocyanines. The p/n bilayers were much more sensitive to ethanol than the corresponding n/p bilayer, even though in both cases the current increases under ethanol [10]. The same devices exhibit a current decrease under ammonia, but both with a very low sensitivity. However, the response observed is not clearly related to the ambipolar character of the devices, since the morphology of sensing material can be different in both structures. In the case of diketopyrrolopyrrole-based ambipolar transistors, the interest of ambipolar character comes from the number of physical parameters to measure, like both electron and hole mobilities, additionally to conductivity [35]. Thus, using a combined pattern-recognition method along with these multiple sensing parameters, a detection down to 40 ppm of xylene and a discrimination between xylene isomers were achieved. These few examples stress the need for studying the interest of ambipolar materials for chemosensing.

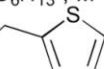
While the interest in ambipolar materials is obvious in organic electronics, it is completely looked over in conductometric sensors. Generally, in sensors, the increase or decrease of the measured electrical current gives a first indication on the nature of chemical species in the atmosphere in contact with the device. This is the reason why we want to discuss the interest of ambipolar materials for gas sensing.

In the present paper, we report on the electrochemical and chemosensing properties of three differently substituted phthalocyanines, the octafluorophthalocyanine Cu(F₈Pc), **1**, the octacarboxylate hexyl ester cobaltphthalocyanine Co((COOC₆H₁₃)₈Pc), **2**, and a recently synthesized phthalocyanine bearing both electron-donating and electron-withdrawing substituents, the zinc tetra-{2-(2-thienyl)ethoxy}-dodecafluorophthalocyanine, Zn(T₄F₁₂Pc), **3**, (Scheme 1) [36]. The conductometric transducer used in this study is a Molecular Semiconductor – Doped Insulator heterojunction, hereafter called MSDI. MSDIs are devices designed and patented by one of the authors [37,38]. They are formed by a thin film-based heterostructure combining a rather poor conducting sublayer in contact with two interdigitated electrodes and a highly conductive top layer made of LuPc₂.



1 $R_1 = H$, $R_2 = R_3 = F$, $M = Cu(II)$

2 $R_1 = H$, $R_2 = R_3 = COOC_6H_{13}$, $M = Co(II)$

3 $R_1 = R_3 = F$, $R_2 = O-CH_2-CH_2-$ , $M = Zn(II)$

Scheme 1 List of the phthalocyanine complexes studied in this work

2. Experimental

2.1. Chemicals.

The 2,3,9,10,16,17,23,24-octafluorinated copper phthalocyanine, $Cu(F_8Pc)$, **1**, was obtained by reaction of 4,5-difluoro-1,2-dibromobenzene with copper cyanide as described previously [37]. The cobalt 2,3,9,10,16,17,23,24-octa(hexyloxy)phthalocyanine, $Co((COOC_6H_{13})_8Pc)$, **2**, was obtained in this work (Suppl. Mater.). The 2,9,16,23-tetra-{2-(2-thienyl)ethoxy}-1,3,4,8,10,11, 15,17,18,22,24,25-dodecafluoro-zinc phthalocyanine, $Zn(T_4F_{12}Pc)$, **3**, was synthesized recently in the ICMUB, by heating the 4-{2-(2-thienyl)ethoxy}-3,5,6-trifluoro-phthalonitrile with zinc acetate, in chloronaphthalene, at 175 °C for 48 h, and purified by successive precipitation and washings [36].

2.2. Characterizations

The UV-visible spectra were registered using a Shimadzu UV-2600 Spectrometer between 350 nm and 800 nm. A bare floated glass substrate was used as a reference for the thin films. The infrared spectra were recorded on a Bruker Vector 22 using KBr pellets, in transmission mode. Mass spectroscopy analysis was performed on an electrospray mass spectrometer amaZon SL (Bruker) coupled with a HPLC Ultimate 3000 RSLC (Dionex).

2.3. Electrochemical measurements

All electrochemical experiments were performed in DMF (dried by percolation on activated alumina) + Bu₄NPF₆ 0.1 M, with a PGSTAT302 N (Metrohm) potentiostat connected to a PC and the data collected were analyzed using the Nova[®] 1.11 Software. Cyclic voltammetry (CV) was carried out by means of a three-electrode configuration consisting of the Pt disk (1.6 mm in diameter, Bioanalytical Systems) as working electrode, a platinum wire as counter-electrode and an SCE electrode as reference separated from the solution by a glass chamber with a porous vycor tip filled up with a saturated solution of Bu₄NPF₆ in DMF. Potentials were reported versus the saturated calomel electrode, SCE. The working Pt electrode was soaked for 10 min in KOH (2 M), polished with 0.1 μm alumina, etched for 10 min in concentrated sulfuric acid (2 M) and sonicated 10 min in water, and then in absolute ethyl alcohol. The solutions were deoxygenated for 10 min with argon, and a positive overpressure of argon was maintained above the electrolyte during the entire measurement performed at room temperature.

2.4. Electrical and chemosensing measurements

Electrical measurements were carried out with Indium Tin Oxide (ITO) interdigitated electrodes (IDE) deposited onto a 1 x 1 cm² glass substrate and separated by 75 μm. Their total length was 15 mm. Thin films of phthalocyanines were prepared either by sublimation under secondary vacuum (ca. 10⁻⁶ mbar) in a UNIVEX 250 thermal evaporator (Oerlikon, Germany), at a rate of 1 Å.s⁻¹, by heating in a temperature range of 400-450 °C for **1** and 450-500 °C for LuPc₂, or by the solvent cast technique, from DMF solutions. The workbench used for NH₃ exposure, at different relative humidity (rh) values, was described previously [39]. Ammonia gas, 1000 ppm in synthetic air and synthetic air were used from standard cylinders, purchased from Air Liquide, France. The total flow was in the range 0.5-0.55 NL.min⁻¹ depending on ammonia concentration and the volume of the test chamber was 8 cm³. Gas sensing experiments were carried out in a dynamic fashion, with 4 min-long rest periods alternating with 1 min-long exposure periods. In the present study, all the electrical

measurements were carried out at the lab temperature (18–22 °C) unless otherwise specified.

3. Results and Discussion

3.1. Electrochemical studies

From the electrochemical data reported for the zinc tetra-{2-(2-thienyl)ethoxy}-phthalocyanine [40], the zinc hexadecafluorophthalocyanine and the non substituted zinc phthalocyanine [41], we estimated the values of redox potentials of **3**. Since from ZnPc (-0.95) to Zn(F₁₆Pc) (-0.43 V), $E_{1/2red}$ is shifted by +0.52 V, due to the presence of 16 fluorine atoms, we can evaluate the effect of twelve F atoms at +0.39 V. In the same way, based on the reduction potential of ZnT₄Pc (-0.99 V vs AgCl/Ag, i.e. ca. -1.03 V vs SCE) and the effect of twelve fluorine atoms, the reduction potential of **3** is expected to lie at ca. -0.65 V (-1.03 +0.38).

The electrochemical behavior of phthalocyanines **2** and **3** was investigated using cyclic voltammetry (CV) in DMF, at a concentration of 10⁻³ mol.L⁻¹ (Figs S4 and S5). Experimentally, **3** exhibits two reduction steps, at -0.78 V (E_{pcred1} , irreversible system) and -1.05 V (reversible system, $E_{1/2red2} = (E_{pcred2} + E_{pared2})/2$) vs SCE, which can be attributed to the successive reductions of the phthalocyanine ring, corresponding to the redox couples Pc²⁻/Pc³⁻ and Pc³⁻/Pc⁴⁻, respectively. Taking into account the irreversibility of the first reduction peak, the E_{pcred1} value at -0.78 V turns out to be compatible with the value above estimated for the first reduction potential (-0.65 V). One oxidation peak attributed to the first oxidation of the phthalocyanine ring appears at +0.97 V (E_{pox1}). Due to the lack of reversibility, it is not possible to define a redox potential difference, ΔE_{redox} , between the first oxidation and reduction potentials.

The cyclic voltammogram of **2** (Fig. S4) reveals 3 redox systems: Two irreversible reduction steps at $E_{red1} = -0.50$ V and $E_{red2} = -1.18$ V vs SCE and one reversible oxidation peak at $E_{1/2ox1} = +0.62$ V [36]. The later system corresponds to the metal oxidation (Co^{III/II}) coordinated to the solvent [42]. The complex is stabilized in DMF compared to CH₂Cl₂ ($E_{1/2ox1} = +0.45$ V) (Fig. S6) in which no solvent coordination occurs, making it more difficult to oxidize.

The electrochemistry of Cu((COOR)₈Pc) was reported for R = octyl, with $E_{ox1} = +1.14$ V and $E_{red1} = -0.49$ V vs SCE [43]. These values are shifted by -0.10 V when two withdrawing

substituents are replaced by one 15C5 crown ether substituent, equivalent to two electron-donating alkoxy groups. So, Cu((COOR)₆(15C5)Pc), hereafter referred to as 15C5, lies very near **3**, with, in both cases, three electron-withdrawing moieties per donating substituent. Considering that one alkoxy group annihilates the effect of one F atom, the electronic properties of **3** should be very similar to those of M(F₈Pc). Additionally, ultraviolet photoelectron spectroscopy (UPS) and inverse emission photoelectron spectroscopy (IEPS) showed that the energy levels of **1** are in between these of CuPc and Cu(F₁₆Pc) [29]. So, the three studied phthalocyanines **1-3** have electrochemical properties close to each other. The three corresponding materials may exhibit an ambipolar behavior under the right conditions. Despite being determined on molecules in electrolytic solutions, electrochemical potentials can be used to evaluate the energy values of the frontier orbitals, HOMOs and LUMOs, known to be responsible for the electronic properties of the corresponding materials, in the solid state. Indeed, it was shown that, in the case of large aromatic molecules, as phthalocyanines, the redox potential difference $\Delta E_{\text{redox}} = E^{\circ}_{\text{ox1}} - E^{\circ}_{\text{red1}}$ does not depend on the polarity and the dielectric constant of the medium in which they are determined, and that there is a good agreement between ΔE_{redox} (in V) and the energy gap (in eV) determined in the solid state [44]. However, determining an absolute energy level in the solid state raises the question of the reference. There is a consensus on calculating the HOMO and LUMO energy values from the onset potential defined as the potential at which the initial electron transfer from the HOMO, or to the LUMO, becomes visible on the cyclic voltammogram as a rise in anodic or cathodic current, respectively [45-48]. So, we calculated the energy of HOMOs and LUMOs of all the above mentioned phthalocyanines from the onset of their redox potentials determined in solution versus SCE or versus ferricinium/ferrocene (Fc⁺/Fc), as reference electrodes, depending on the reference actually used to determine the redox potentials:

$$E_{\text{HOMO}} = -(E_{\text{onset/SCE}}^{\text{ox}} + 4.4) \quad (1a) \text{ or } E_{\text{HOMO}} = -(E_{\text{onset/Fc}}^{\text{ox}} + 4.84) \quad (1b)$$

$$E_{\text{LUMO}} = -(E_{\text{onset/SCE}}^{\text{red}} + 4.4) \quad (2a) \text{ or } E_{\text{LUMO}} = -(E_{\text{onset/Fc}}^{\text{red}} + 4.84) \quad (2b)$$

In the present work, the standard redox potential of Fc⁺/Fc was determined at +0.44 V vs SCE. All the data are compiled in Table 1 and reported in Fig. 1. The energy levels of a series

of copper phthalocyanines determined directly versus the vacuum level, by Ultra-Violet Photoelectron Spectroscopy (UPS) and Inverse PhotoEmission Spectroscopy (IEPS), have been added [29]. For all the data reported in literature without showing voltammograms, the $E_{1/2}$ was used instead of the onset values.

Table 1: Redox potentials of a series of phthalocyanines determined by cyclic voltammetry versus SCE (peak potentials or $E_{1/2}$ if indicated), and energy values of HOMOs and LUMOs calculated from the onset of these potentials (or from peak potentials or $E_{1/2}$ if indicated), using equations 1 and 2, or directly determined by photoelectron spectroscopies, UPS and IEPS.

Compound [ref.]	Solvent	E_{red2} (V)	E_{Red1} (V)	E_{Ox1} (V)	LUMO (eV)	HOMO (eV)
Zn(T ₄ Pc) [40]	DMF		-1.03 ^a	0.43 ^a $E_{1/2}$	-3.37 ^f	-4.83 ^f
ZnPc [41]	DMF	-1.35 $E_{1/2}$	-0.95 $E_{1/2}$	0.59 $E_{1/2}$	-3.45 ^f	-4.99 ^f
[49]	DMF	-1.42 $E_{1/2}$	-0.93 $E_{1/2}$	0.64 $E_{1/2}$		
Zn(T ₄ F ₁₂ Pc), 3 [36]	DMF	-1.05 $E_{1/2}$	-0.78	0.97	-3.62 ^f	-5.37 ^f
This work					-4.14	-5.19
Co((COOC ₆ H ₁₃) ₈ Pc), 2	DMF	-1.18	-0.50	0.62 $E_{1/2}$ ^b	-3.90 ^f	
This work					-4,24	
Cu((COOC ₈ H ₁₇) ₈ Pc) [43]	CH ₂ Cl ₂	-0.81	-0.49	1.14	-3.95 ^e	-5.58 ^e
15C5 ^d [43]	CH ₂ Cl ₂	-0.85	-0.59	1.05	-3.85 ^e	-5.49 ^e
Zn(F ₁₆ Pc) [41]	DMF	-0.64 $E_{1/2}$	-0.43 $E_{1/2}$	1.04 ^e	-3.97 ^f	-5.44 ^f
[49]		-0.9 $E_{1/2}$	-0.6 $E_{1/2}$		-3.47	
CuPc [29]					-3.16 ^g	-5.20 ^g
Cu(F ₈ Pc), 1 [29]					-3.91 ^g	-6.06 ^g
Cu(F ₁₆ Pc) [29]					-4.46 ^g	-6.39 ^g

^aRecalculated from data determined vs AgCl/Ag, using ($E_{AgCl/Ag}^0 = -0.04V$ vs SCE).

^bThis oxidation corresponds to the redox couple Co^{3+}/Co^{2+} .

^cValues given in ref. [43] using a slightly different formula.

^dAcronym used for Cu((COOR)₆(15C5)Pc).

^eEstimated in ref. [41] from an irreversible peak.

^fDetermined from equations 1 or 2 in which $E_{1/2}$ or E_{peak} were used instead of E_{onset} .

^gMeasured experimentally by photoelectron spectroscopy (UPS and IEPS) [29].

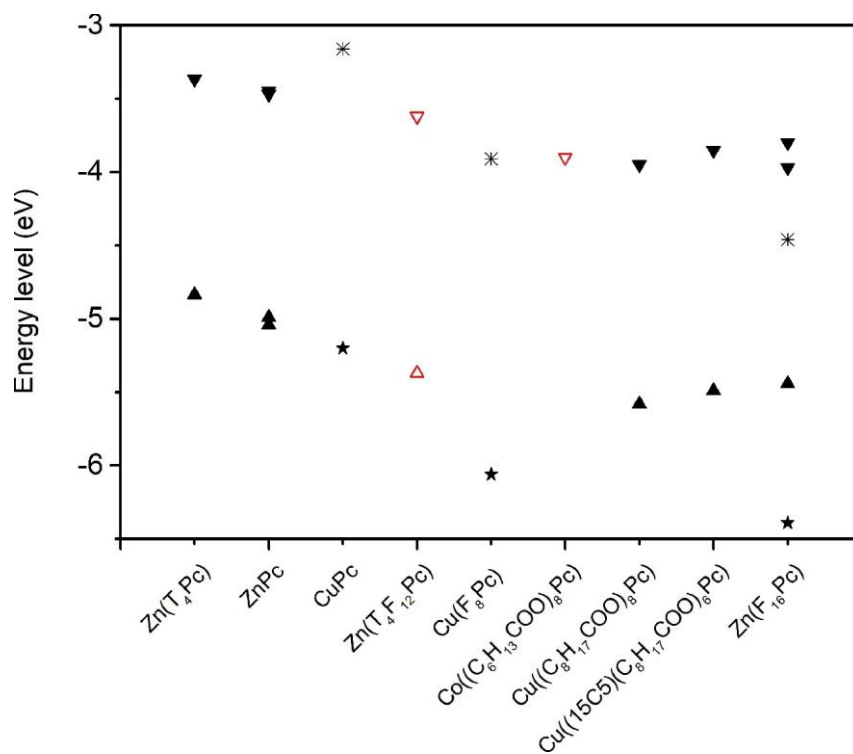


Figure 1: Energy values of HOMO and LUMO calculated from redox potentials determined by cyclic voltammetry versus SCE (triangle), using equations 1 and 2, or directly determined by photoelectron spectroscopies UPS and IEPS, on the copper complexes (star).

3.2. Electrical and sensing properties

Films of **2** and **3** were obtained by solvent cast, from 85 μL of DMF solutions, at concentrations of 2×10^{-3} and 3.3×10^{-3} mol L^{-1} , respectively, deposited dropwise on interdigitated electrodes (IDE). The substrate was heated at 60 $^{\circ}\text{C}$ in a closed desiccator in order to fully evaporate the solvent and increase the homogeneity of the films. Electrical measurement in ambient atmosphere showed that these films were too resistive for suitable chemosensing studies, at least up to +10 V, with these IDEs. However, it was possible to build MSDI heterojunctions, by vacuum evaporation of lutetium bisphthalocyanine, LuPc_2 , 50 nm in thickness, on the previous films. For **1**, the sublayer (50 nm in thickness) was also deposited by vacuum evaporation. The MSDI heterojunctions are called hereafter MSDI 1, MSDI 2 and MSDI 3, in reference to the nature of their sublayer. Their electronic absorption spectra in UV-visible are given in supplementary materials (Figs S1, S2 and S3).

For pure n-type sublayers, such as metalloperfluorophthalocyanines $\text{M}(\text{F}_{16}\text{Pc})$, the response to ammonia is positive whereas it decreases for a LuPc_2 resistor. On the contrary, with pure p-type sublayers, e.g. pentacene, oligothiophene or a non

substituted phthalocyanine [37,50], ammonia induces a decrease in current through the MSDI. An important point about MSDIs is that the only material available to interact with the outer atmosphere is the top layer. We demonstrated that the transport properties are dominated not only by the energy barrier at the interface between the sublayer and the LuPc₂ top layer, but also by the Schottky contact between the sublayer and the electrodes [51]. These energy barriers are higher with M(F₁₆Pc) than with p-type sublayers.

The I-V characteristics measured on all three MSDIs are symmetrical but not linear (Fig. 2), contrarily to those observed with a LuPc₂ resistor in the same potential range [37]. The deviation from the linearity is weak for MSDI 2, but greater for MSDIs 1 and 3. The current measured at 10 V under dry synthetic air varies by less than a factor of ten for all three devices, from 6.6 μA for MSDI 3, to 16.3 μA for MSDI 1 and to 53 μA for the MSDI 2.

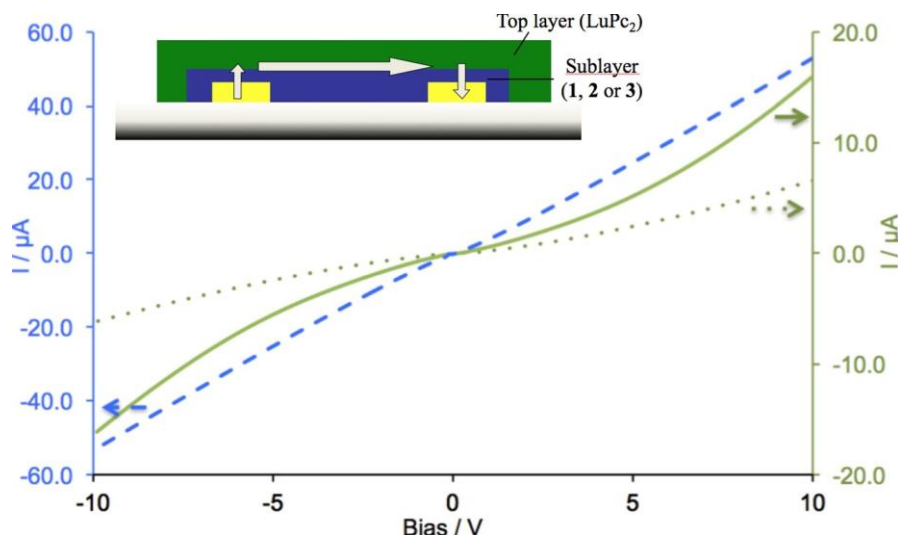


Figure 2. Typical I-V characteristics for the MSDIs 1 (solid line), 2 (dashed line), and 3 (dotted line) prepared with compounds **1**, **2** and **3** as sublayer, respectively, and with LuPc₂ as a top layer. Inset: Scheme of a MSDI heterojunction; the arrows indicate the pathway of charges across the device.

Under NH₃, the MSDI 3 showed a current decrease (Fig. 3), as expected for a p-type MSDI heterojunction prepared from a p-type sublayer. This reveals that compound **3** is capable of transporting positive majority charge carriers, even though their density remains very low. This was not obvious *a priori* due to the presence of twelve fluorine atoms on the phthalocyanine ring. This confirms that the four electron-donating alkoxy groups compensate, at least partially, the withdrawing effect of fluorine atoms, as mentioned in the electrochemistry section above. Quantitatively, the

relative response, defined as $(I-I_0)/I_0$ is of -1.6 % at 30 ppm NH_3 , under dry atmosphere.

The MSDI 2 exhibits also a negative response to NH_3 (-0.7 % at 30 ppm) under dry atmosphere, i.e. less than half that of the MSDI 3.

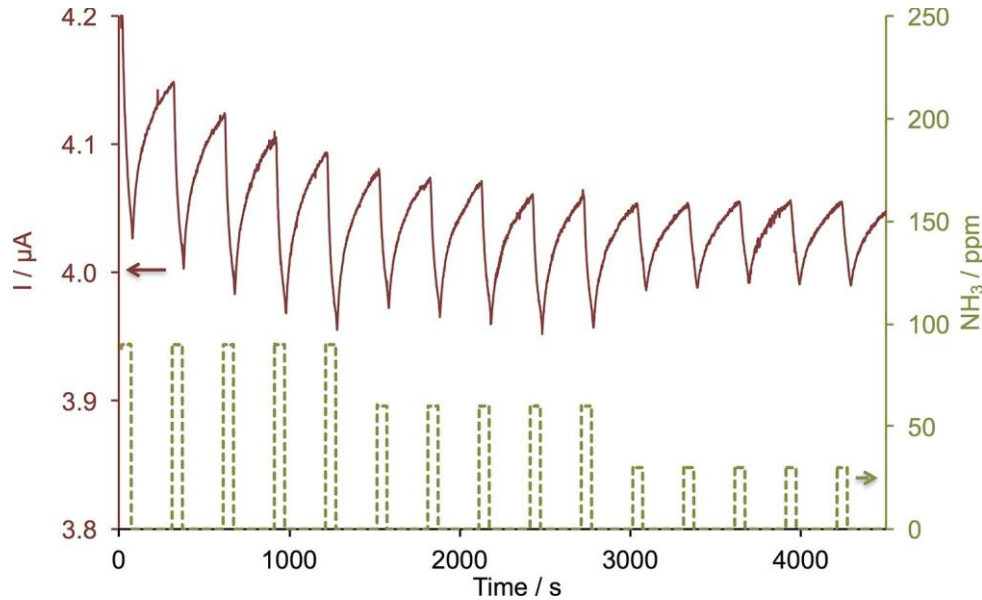


Figure 3: Response of a MSDI 3 to NH_3 (90, 60 and 30 ppm), in dry atmosphere, during exposure/recovery cycles (1 min/4 min); $T = 21\text{ }^\circ\text{C}$.

Contrarily to their response to NH_3 , the MSDIs 2 and 3 exhibit very different responses to humidity. In order to compare their sensitivity, we plotted the I/I_0 values as a function of time in the range 10-70 % rh, I_0 being the current value at the beginning of the experiment (Fig. 4). During the first exposure to 70% rh, the current of the MSDI 3 decreases by 6% in 10 min, whereas it diminishes by only 0.9% for the MSDI 2. More interestingly, for the MSDI 2, no matter the history of the sample, such as several exposition periods to humidity and ammonia, the increase of rh from 0 to 70 % induces a current decrease of ca. 2%. In the case of the MSDI 3, the relative response to humidity variations is highly dependent on the history of the device, and lies in the range -5% to -10%, for the same experiment in the range 10-70% of rh.

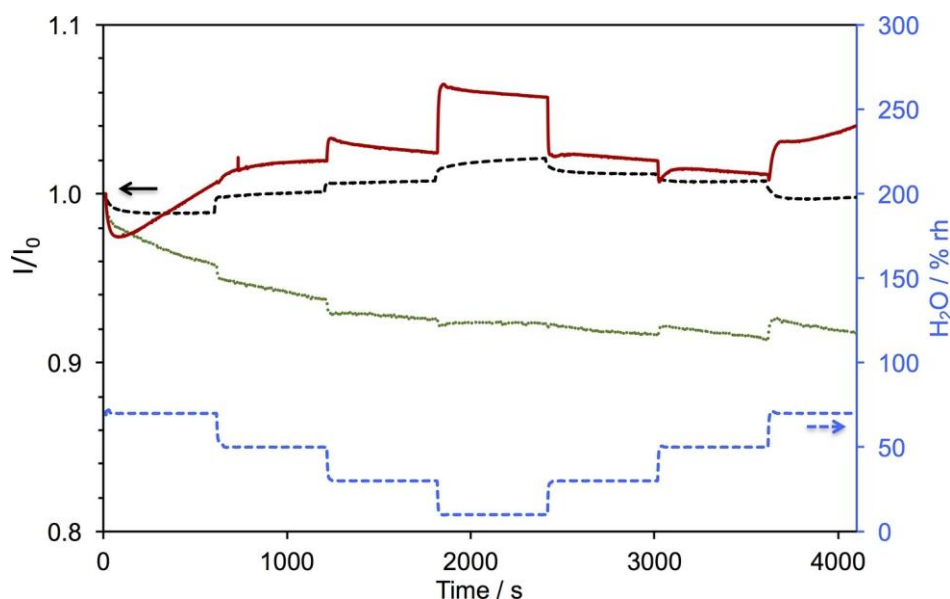


Figure 4: Response I/I_0 of MSDIs 1 (solid line), 2 (dashed line) and 3 (dotted line) to relative humidity in the range 10-70 % (bottom curve), during exposure periods of 10 min. I_0 is the current value of each device at the beginning of the experiment.

We also studied the sensitivity of all the devices to NH_3 , at 90, 60 and 30 ppm, and under a variable relative humidity level, in the range 10-70 % rh. For the MSDI 2, the response to NH_3 is highly reversible in all the rh range, even though a drift of the response occurs at 70 % (Fig. 5). Despite the clearly visible response to NH_3 , the overall current variation caused by the rh variations, which is of -3 % between 10 % rh and 70 % rh, remains higher than the response to NH_3 . It is precisely the double of the response to 90 ppm NH_3 (-1.5 %). However, we have to keep in mind that ammonia sensors that are not affected by humidity variations in such a broad range are very rare [52,53]. As such, MSDI 2 exhibits an interesting response to NH_3 for all application in which the rh remains in the range 30-50 %. Despite a higher response to NH_3 , the behavior of MSDI 3 is worse in such a competitive experiment. Thus, the response to 90 ppm NH_3 is ca. 3%, whereas the current decreases by 20% from 10 % rh to 70 % rh. As a result, the MSDI 2 reveals to be a better NH_3 sensor than the MSDI 3 when targeting real-world conditions, and can be used when the relative humidity is known or when it varies in a small range (typically in the range 30-50 % rh).

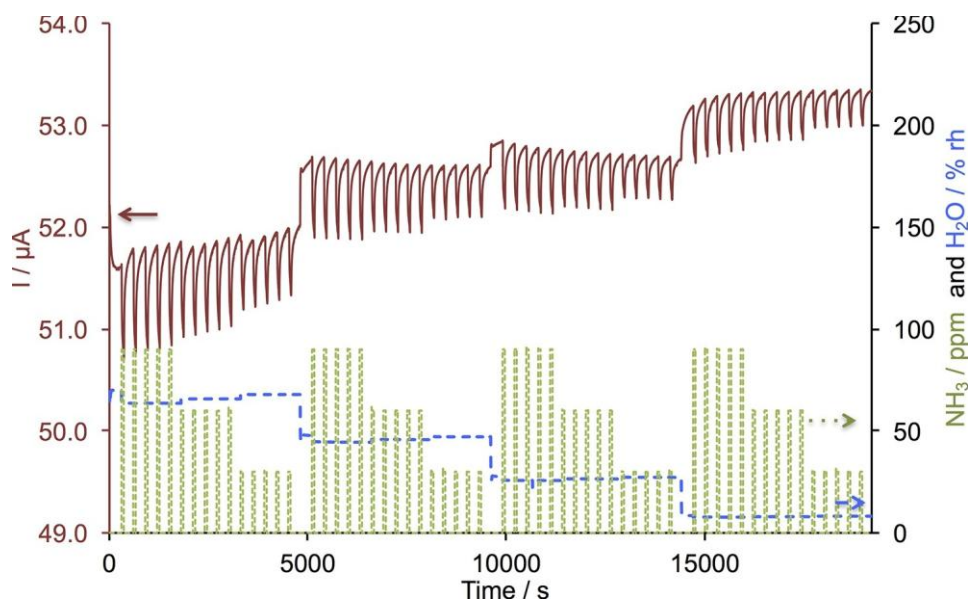


Figure 5: Response of a MSDI 2 (solid line) to NH_3 (90, 60 and 30 ppm, dotted line), with relative humidity in the range 10-70 % (dashed line), during exposure/recovery cycles (1 min/4 min); $T = 20\text{ }^\circ\text{C}$.

The chemosensing properties of MSDIs 1 are different from those of MSDIs 2 and 3. In dry air, the current decreases under NH_3 , just as it does for the two other devices built with a p-type sublayer. But, during the first exposure to 70 % of rh, the current sharply decreases by 5% at first, down to a minimum value, then sharply increases to revert back to its original value (Fig. 6). Such transient behavior was observed at every new exposure to humidity that followed a long period in dry air. This means that the humidity is not only trapping or neutralizing majority charge carriers as expected for a p-type transducer, but we believe that this MSDI turns from p-type to n-type majority charge carriers. This is due to the very peculiar behavior of the LuPc_2 top layer, which is a p-type material in air but is also capable of transporting negative charge carriers [3]. As a result, when a LuPc_2 top layer is associated with **1** as a sublayer, the majority charge carriers responsible for the current turn from positive to negative. This is allowed by the value of the energy levels of **1**. So, a small difference in the frontier orbitals energy between **1**, **2** and **3** is responsible for strong effects in chemosensing. This fact is confirmed by exposure to NH_3 at different relative humidity values. During exposition, the measured current through MSDI 1, at 70 % and 50 % rh, increases under NH_3 whereas it decreases at 30 % and 10 % rh (Fig. 7). Quantitatively, the relative response to 30 ppm NH_3 is +3.7 % at 70 % rh and +1.5 % at 50 % rh, but turns

to negative values at 30 % rh (-1.4%) and at 10 % rh (-1.6%). In air the MSDI 1 exhibits a p-type behavior, but water molecules trap majority (positive) charge carriers in the top layer when the humidity increases: the current is governed by minority (negative) mobile charges and the device behaves as a typical n-type MSDI, with an increase of the current under NH_3 . These results confirm the ambipolar behavior of the MSDI 1.

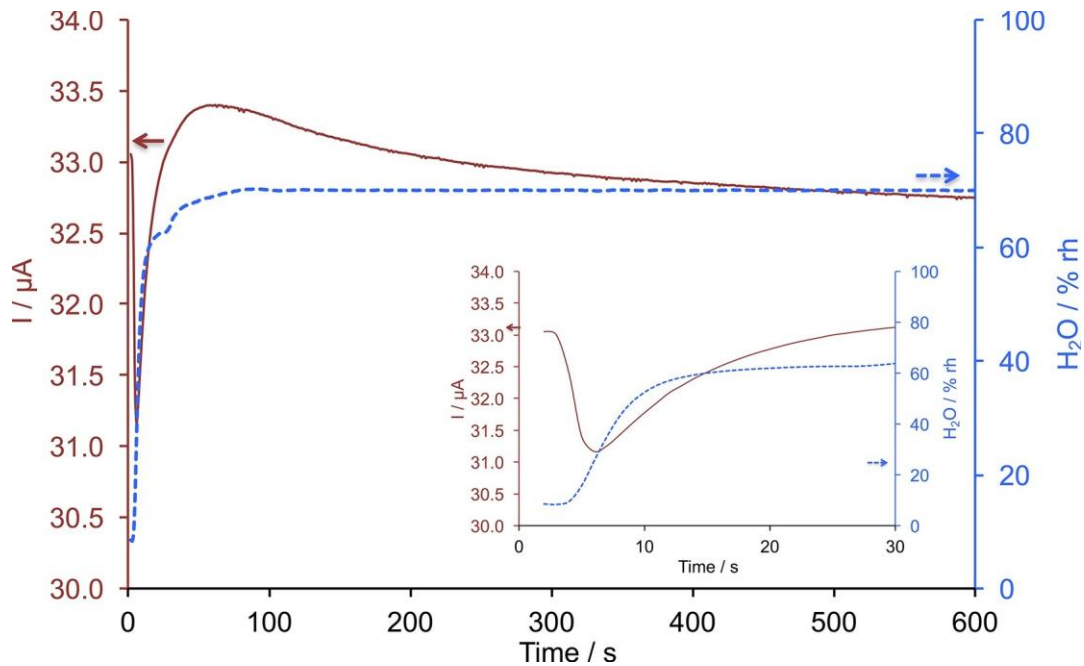


Figure 6: Variation of the current (solid line) as a function of time for MSDI 1 during exposure to relative humidity (dotted line).

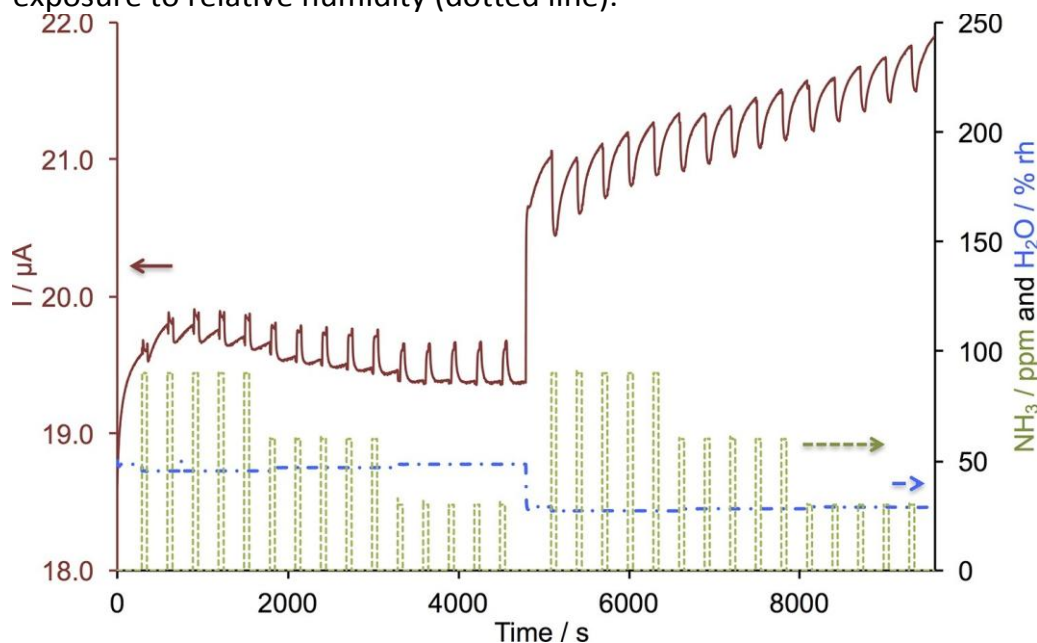


Figure 7: Response of MSDI 1 (solid line) to NH_3 (90, 60 and 30 ppm, dotted line), with rh values of 50 % and 30 % (dashed line), during exposure/recovery cycles (1 min/4 min); $T = 19\text{ }^\circ\text{C}$.

Such a transient behavior had been already mentioned for MSDI 1, when exposed to 90 ppb of ozone, a strong oxidizing species, but without any reference to a possible ambipolar behavior [37]. In the very beginning of the exposure, the sensor displays an increase of current due to the doping of LuPc_2 , as any p-type conductometric device. However, the conductivity profile reaches a maximum in the subsequent seconds, then the current drops (Suppl. Info. of [37]).

In addition, we repeated the exposure to a given NH_3 concentration and a given rh value for twenty exposure/recovery cycles. The current variation at rh values of 70 % and 30 %, both at 30 ppm NH_3 are shown on Fig. 8 left. At 70 % rh, the sensor remains of n-type, even though the relative response decreases from -7.3 % to -4.9 % along the experiment. At 30 % rh, the relative response is more stable, at 1.62 ± 0.05 %.

In another experiment, following a 15 min long exposition, the sensor recovers its baseline current after about 1 h, as demonstrated by exposing MSDI 1 to 30 ppm NH_3 at 30 % rh (Fig. 8 right). This experiment shows that the response after 15 min is about 7 times higher than the one observed after the 1 min long exposures.

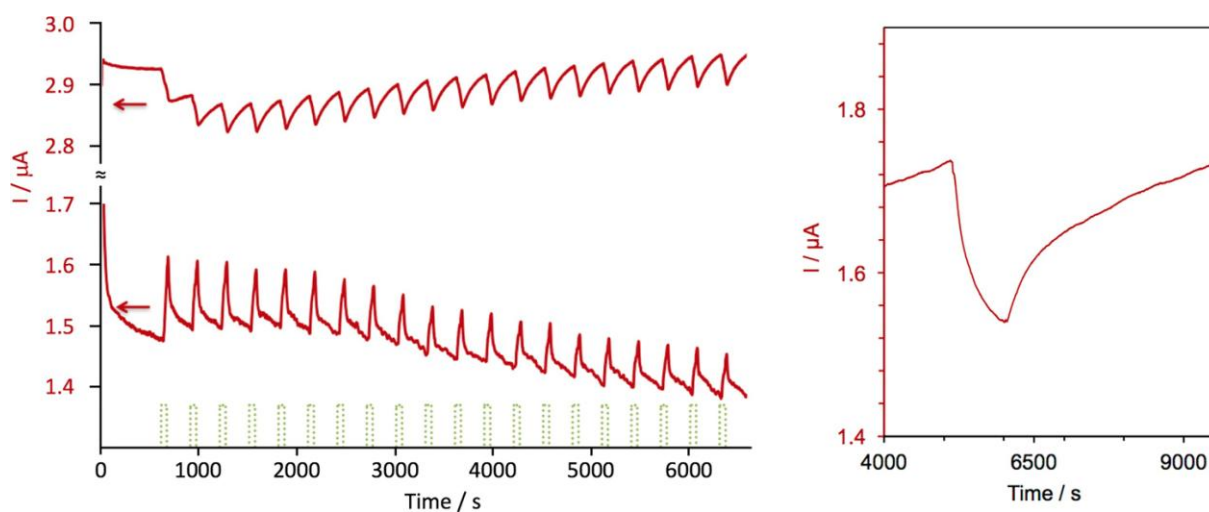


Figure 8: (left) Response of a MSDI 1 (solid line) to 30 ppm NH_3 (dotted line) at a relative humidity value of 30 % (upper curve) and 70 % (lower curve), during twenty exposure/recovery cycles (1 min/4 min); (right) response to 30 ppm of NH_3 (exposure duration: 15 min) at 50 % rh; $T = 20$ °C.

At a first glance, the response of MSDI 1 to NH_3 seems quite bad, since it is positive or negative depending on the relative humidity value. However, if the rh is stable, or known, e.g. by combining the MSDI device with a humidity sensor, it can be used as a NH_3 sensor. The association of two of the sensors studied here is even more

interesting: for instance, if MSDIs 1 and 3 (or 1 and 2) were to be combined into one sensing system, a principal component analysis of the data would take advantage of the differences in their responses to give access to both the concentration of NH₃ and the rh value. So, the ambipolar behavior of the conductometric sensor enables a multimodal detection, as above mentioned in the introduction with polymer-based ambipolar transistors [35].

4. Conclusion

The electrical properties of three substituted phthalocyanines bearing electron withdrawing substituents have been studied. The octafluorophthalocyanine **1**, the octaester phthalocyanine **2** and the phthalocyanine bearing four alkoxy groups and twelve fluorine atoms **3** exhibit almost similar electrochemical properties. Used as sublayers in MSDI heterojunctions with LuPc₂ as a top layer, they show quite different chemosensing features. MSDIs 2 and 3 exhibit a negative response to ammonia, whereas the response of the MSDI 1 depends on the relative humidity. We showed that this particular behavior results from the ambipolar character of **1**.

Since the response of the device exposed to one gas can be positive or negative depending on the environmental conditions, such as a humidity variation in the present study, the ambipolar behavior of a conductometric chemical sensor can be considered as an unacceptable parameter to get a working and efficient sensor. However, it can be also considered as a feature that makes these ambipolar devices stand out from all other conductometric devices. This makes them promising elements for the design of new sensor arrays. Since the ambipolar behavior of a semiconductor material depends on the operating conditions, ambipolar materials, i.e. materials capable of exhibiting both p-type and n-type conductivities, are *a priori* good candidates to building in such sensing systems.

Acknowledgements

The authors acknowledge the *Agence Nationale de la Recherche* for funding through the ANR projects CAP-BTX ANR-BLAN-2010-917-02 and OUTSMART ANR-2015-CE39-0004-03 and the MENESR for a PhD grant (A. W.). Financial support from the European Union and the *Conseil Régional de Bourgogne* through the FABER and the

PARI SMT 08 and CDEA programs is gratefully acknowledged. We would like to thank the European Union for fundings (FEDER and short term missions) through the COST action TD1105 EuNetAir. The research Ministry in Burkina Faso is thanked for supporting a mission in France (S. O.).

References

- [1] Y. Zhao, Y. Guo, Y. Liu, 25th Anniversary article: Recent advances in n-type and ambipolar organic field-effect transistors, *Adv. Mater.* 25 (2013) 5372–5391. doi:10.1002/adma.201302315.
- [2] J. Zaumseil, H. Sirringhaus, Electron and ambipolar transport in organic field-effect transistors, *Chem. Rev.* 107 (2007) 1296–1323. doi:10.1021/cr0501543.
- [3] G. Guillaud, M. Al Sadoun, M. Maitrot, J. Simon, M. Bouvet, Field-effect transistors based on intrinsic molecular semiconductors, *Chem. Phys. Lett.* 167 (1990) 503–506.
- [4] J.-J. André, K. Holczer, P. Petit, M.-T. Riou, C. Clarisse, R. Even, et al., Electrical and magnetic properties of thin films and single crystals of bis(phthalocyaninato)lutetium, *Chem. Phys. Lett.* 115 (1985) 463–466. doi:10.1016/0009-2614(85)85171-X.
- [5] M. Bouvet, J. Simon, Electrical properties of rare earth bisphthalocyanine and bisnaphthalocyanine complexes, *Chem. Phys. Lett.* 172 (1990) 299–302. doi:10.1016/0009-2614(90)85407-4.
- [6] E.J. Meijer, D.M. de Leeuw, S. Setayesh, E. van Veenendaal, B.H. Huisman, P.W.M. Blom, et al., Solution-processed ambipolar organic field-effect transistors and inverters, *Nat. Mater.* 2 (2003) 678–682. doi:10.1038/nmat978.
- [7] H. Shim, A. Kumar, H. Cho, D. Yang, A.K. Palai, S. Pyo, Laterally-stacked, solution-processed organic microcrystal with ambipolar charge transport behavior, *ACS Appl. Mater. Interfaces.* 6 (2014) 17804–17814. doi:10.1021/am5044505.
- [8] M. Jea, A. Kumar, H. Cho, D. Yang, H. Shim, A.K. Palai, et al., An organic microcrystal array-embedded layer: highly directional alternating p- and n-channels for ambipolar transistors and inverters, *J. Mater. Chem. C.* 2 (2014) 3980–3987. doi:10.1039/c4tc00042k.
- [9] A. Babel, J.D. Wind, S.A. Jenekhe, Ambipolar charge transport in air-stable polymer blend thin-film, *Adv. Funct. Mater.* 14 (2004) 891–898. doi:10.1002/adfm.200305180.
- [10] Y. Wu, P. Ma, N. Wu, X. Kong, M. Bouvet, X. Li, et al., Two-step solution-processed two-component bilayer phthalocyaninato copper-based heterojunctions with interesting ambipolar organic transiting and ethanol-sensing properties, *Adv. Mater. Interfaces.* 3 (2016) 1600253. doi:10.1002/admi.201600253.
- [11] H. Sirringhaus, Device physics of solution-processed organic field-effect transistors, *Adv. Mater.* 17 (2005) 2411–2425. doi:10.1002/adma.200501152.
- [12] J. Cornil, J.L. Brédas, J. Zaumseil, H. Sirringhaus, Ambipolar transport in organic conjugated materials, *Adv. Mater.* 19 (2007) 1791–1799. doi:10.1002/adma.200602922.
- [13] H. Wang, D. Yan, Organic heterostructures in organic field-effect transistors, *NPG Asia Mater.* 2 (2010) 69–78. doi:10.1038/asiamat.2010.44.
- [14] T.D. Anthopoulos, C. Tanase, S. Setayesh, E.J. Meijer, J.C. Hummelen, P.W.M. Blom, et al., Ambipolar organic field-effect transistors based on a solution-processed

- methanofullerene, *Adv. Mater.* 16 (2004) 2174–2179. doi:10.1002/adma.200400309.
- [15] T. Lei, J.-H. Dou, X.-Y. Cao, J.-Y. Wang, J. Pei, A BDOPV-based donor-acceptor polymer for high-performance n-type and oxygen-doped ambipolar field-effect transistors, *Adv. Mater.* 25 (2013) 6589–6593. doi:10.1002/adma.201302278.
- [16] H. Chen, Y. Guo, Z. Mao, G. Yu, J. Huang, Y. Zhao, et al., Naphthalenediimide-based copolymers incorporating vinyl-linkages for high-performance ambipolar field-effect transistors and complementary-like inverters under air, *Chem. Mater.* 25 (2013) 3589–3596. doi:10.1021/cm401130n.
- [17] X. Kong, Q. Jia, F. Wu, Y. Chen, Flexible, ambipolar organic field-effect transistors based on the solution-processed films of octanaphthoxy-substituted bis(phthalocyaninato) europium, *Dyes Pigments.* 115 (2015) 67–72. doi:10.1016/j.dyepig.2014.12.002.
- [18] J. Kan, Y. Chen, D. Qi, Y. Liu, J. Jiang, High-performance air-stable ambipolar organic field-effect transistor based on tris(phthalocyaninato) europium(III), *Adv. Mater.* 24 (2012) 1755–1758. doi:10.1002/adma.201200006.
- [19] X. Kong, X. Zhang, D. Gao, D. Qi, Y. Chen, J. Jiang, Air-stable ambipolar field-effect transistor based on a solution-processed octanaphthoxy-substituted tris(phthalocyaninato) europium semiconductor with high and balanced carrier mobilities, *Chem. Sci.* 6 (2015) 1967–1972. doi:10.1039/C4SC03492A.
- [20] M.L. Tang, A.D. Reichardt, N. Miyaki, R.M. Stoltenberg, Z. Bao, Ambipolar, high performance, acene-based organic thin film transistors, *J. Am. Chem. Soc.* 130 (2008) 6064–6065. doi:10.1021/ja8005918.
- [21] Z. Liang, Q. Tang, R. Mao, D. Liu, J. Xu, Q. Miao, The position of nitrogen in N-heteropentacenes matters, *Adv. Mater.* 23 (2011) 5514–5518. doi:10.1002/adma.201103759.
- [22] W.-J. Zeng, X.-Y. Zhou, X.-J. Pan, C.-L. Song, H.-L. Zhang, High performance CMOS-like inverter based on an ambipolar organic semiconductor and low cost metals, *AIP Advances.* 3 (2013) 012101. doi:10.1063/1.4774287.
- [23] S. Watanabe, T. Fujita, J.-C. Ribierre, K. Takaishi, T. Muto, C. Adachi, et al., Microcrystallization of a solution-processable organic semiconductor in capillaries for high-performance ambipolar field-effect transistors, *ACS Appl. Mater. Interfaces.* 8 (2016) 17574–17582. doi:10.1021/acsami.5b12713.
- [24] J. Li, X. Qiao, Y. Xiong, H. Li, D. Zhu, Five-ring fused tetracyanothienoquinoids as high-performance and solution-processable n-channel organic semiconductors: effect of the branching position of alkyl chains, *Chem. Mater.* 26 (2014) 5782–5788. doi:10.1021/cm502952u.
- [25] H. Usta, C. Risko, Z. Wang, H. Huang, M.K. Delimeroglu, A. Zhukhovitskiy, et al., Design, synthesis, and characterization of ladder-type molecules and polymers. Air-stable, solution-processable n-channel and ambipolar semiconductors for thin-film transistors via experiment and theory, *J. Am. Chem. Soc.* 131 (2009) 5586–5608. doi:10.1021/ja809555c.
- [26] H. Usta, A. Facchetti, T.J. Marks, n-Channel semiconductor materials design for organic complementary circuits, *Acc. Chem. Res.* 44 (2011) 501–510. doi:10.1021/ar200006r.
- [27] Y. Chen, D. Li, N. Yuan, J. Gao, R. Gu, G. Lu, et al., Tuning the semiconducting nature of bis(phthalocyaninato) holmium complexes via peripheral substituents, *J. Mater. Chem.* 22 (2012) 22142–22149. doi:10.1039/c2jm35219b.
- [28] J. Mei, Z. Bao, Side chain engineering in solution-processable conjugated polymers, *Chem. Mater.* 26 (2014) 604–615. doi:10.1021/cm4020805.

- [29] R. Murdey, N. Sato, M. Bouvet, Frontier electronic structures in fluorinated copper phthalocyanine thin films studied using ultraviolet and inverse photoemission spectroscopies, *Mol. Cryst. Liq. Cryst.* 455 (2006) 211–218. doi:10.1080/15421400600698469.
- [30] R.D. Yang, J. Park, C.N. Colesniuc, I.K. Schuller, J.E. Royer, W.C. Trogler, et al., Analyte chemisorption and sensing on n- and p-channel copper phthalocyanine thin-film transistors, *J. Chem. Phys.* 130 (2009) 164703–9. doi:10.1063/1.3078036.
- [31] H. Wang, J. Wang, H. Huang, X. Yan, D. Yan, Organic heterojunction with reverse rectifying characteristics and its application in field-effect transistors, *Org. Electron.* 7 (2006) 369–374. doi:10.1016/j.orgel.2006.04.004.
- [32] I. Muzikante, V. Parra, R. Dobulans, E. Fonavs, J. Latvels, M. Bouvet, A novel gas sensor transducer based on phthalocyanine heterojunction devices, *Sensors.* 7 (2007) 2984–2996. doi:10.3390/s7112984.
- [33] F.I. Bohrer, C.N. Colesniuc, J. Park, M.E. Ruidiaz, I.K. Schuller, A.C. Kummel, et al., Comparative gas sensing in cobalt, nickel, copper, zinc, and metal-free phthalocyanine chemiresistors, *J. Am. Chem. Soc.* 131 (2009) 478–485. doi:10.1021/ja803531r.
- [34] S. Dutta, S.D. Lewis, A. Dodabalapur, Hybrid organic/inorganic ambipolar thin film transistor chemical sensor, *Appl. Phys. Lett.* 98 (2011) 213504. doi:10.1063/1.3583594.
- [35] B. Wang, T.-P. Huynh, W. Wu, N. Hayek, T.T. Do, J.C. Cancilla, et al., A highly sensitive diketopyrrolopyrrole-based ambipolar transistor for selective detection and discrimination of xylene isomers, *Adv. Mater.* 28 (2016) 4012–4018. doi:10.1002/adma.201505641.
- [36] A. Wannebroucq, R. Meunier-Prest, J.-C. Chambron, C.-H. Brachais, J.-M. Suisse, M. Bouvet, *RSC Adv.*, 7 (2017) 41272–41281.
- [37] V. Parra, J. Brunet, A. Pauly, M. Bouvet, Molecular semiconductor-doped insulator (MSDI) heterojunctions: an alternative transducer for gas chemosensing, *Analyst.* 134 (2009) 1776–1778. doi:10.1039/b906786h.
- [38] V. Parra, M. Bouvet, Semiconductor transducer and its use in a sensor for detecting electron-donor or electron-acceptor species, patent US8450725 B2, 2013.
- [39] P. Gaudillat, A. Wannebroucq, J.-M. Suisse, M. Bouvet, Bias and humidity effects on the ammonia sensing of perylene derivative/lutetium bisphthalocyanine MSDI heterojunctions, *Sens. Actuators: B. Chem.* 222 (2016) 910–917. doi:10.1016/j.snb.2015.09.015.
- [40] J. Obirai, T. Nyokong, Synthesis, electrochemical and electrocatalytic behaviour of thiophene-appended cobalt, manganese and zinc phthalocyanine complexes, *Electrochim. Acta.* 50 (2005) 5427–5434. doi:10.1016/j.electacta.2005.03.024.
- [41] B. Schöllhorn, J.P. Germain, A. Pauly, C. Maleysson, J.P. Blanc, Influence of peripheral electron-withdrawing substituents on the conductivity of zinc phthalocyanine in the presence of gases. Part 1: reducing gases, *Thin Solid Films.* 326 (1998) 245–250. doi:10.1016/S0040-6090(98)00553-7.
- [42] M. L'Her, A. Pondaven, Electrochemistry of Phthalocyanines, in *The Porphyrin Handbook*, K.M. Kadish, K.M. Smith, R. Guilard (Eds.), Elsevier, Amsterdam, 2003: vol. 16, pp. 117–169. doi:10.1016/B978-0-08-092390-1.50009-6.
- [43] P. Ma, J. Kan, Y. Zhang, C. Hang, Y. Bian, Y. Chen, et al., The first solution-processable n-type phthalocyaninato copper semiconductor: tuning the semiconducting nature via peripheral electron-withdrawing octyloxycarbonyl substituents, *J. Mater. Chem.* 21 (2011) 18552–18559. doi:10.1039/c1jm13082j.

- [44] M. Bouvet, E.A. Silinsh, J. Simon, Determination of energy gap values in molecular crystals II. Intrinsic dark conductivity and electrochemical methods, *Mol. Mater.* 5 (1995) 255–277.
- [45] M.M. Ahmida, S.H. Eichhorn, Measurements and prediction of electronic properties of discotic liquid crystalline triphenylenes and phthalocyanines, in: 216th ECS Meeting, ECS, 2010: pp. 1–10. doi:10.1149/1.3314449.
- [46] C.M. Cardona, W. Li, A.E. Kaifer, D. Stockdale, G.C. Bazan, Electrochemical considerations for determining absolute frontier orbital energy levels of conjugated polymers for solar cell applications, *Adv. Mater.* 23 (2011) 2367–2371. doi:10.1002/adma.201004554.
- [47] J.L. Brédas, R. Silbey, D.S. Boudreaux, R.R. Chance, Chain-length dependence of electronic and electrochemical properties of conjugated systems: polyacetylene, polyphenylene, polythiophene, and polypyrrole, *J. Am. Chem. Soc.* 105 (1983) 6555–6559. doi:10.1021/ja00360a004.
- [48] L. Leonat, G. Sbârcea, I.V. Branzoi, Cyclic voltammetry for energy levels estimation of organic materials, *UPB Sci. Bull. Ser. B.* (2013).
- [49] K. Hesse, D. Schlettwein, Spectroelectrochemical investigations on the reduction of thin films of hexadecafluorophthalocyaninatozinc (F₁₆PcZn), *J. Electroanal. Chem.* 476 (1999) 148–158. doi:10.1016/S0022-0728(99)00381-2.
- [50] M. Bouvet, H. Xiong, V. Parra, Molecular semiconductor-doped insulator (MSDI) heterojunctions: Oligothiophene/bisphthalocyanine (LuPc₂) and perylene/bisphthalocyanine as new structures for gas sensing, *Sens. Actuators: B. Chem.* 145 (2010) 501–506. doi:10.1016/j.snb.2009.12.064.
- [51] M. Bouvet, P. Gaudillat, A. Kumar, T. Sauerwald, M. Schüller, A. Schütze, et al., Revisiting the electronic properties of Molecular Semiconductor – Doped Insulator (MSDI) heterojunctions through impedance and chemosensing studies, *Org. Electron.* 26 (2015) 345–354. doi:10.1016/j.orgel.2015.07.052.
- [52] T. Sizun, T. Patois, M. Bouvet, B. Lakard, Microstructured electrodeposited polypyrrole–phthalocyanine hybrid material, from morphology to ammonia sensing, *J. Mater. Chem.* 22 (2012) 25246–8. doi:10.1039/c2jm35356c.
- [53] P. Gaudillat, J.-M. Suisse, M. Bouvet, Humidity insensitive conductometric sensors for ammonia sensing, *Key Eng. Mater.* 605 (2014) 181–184. doi:10.4028/www.scientific.net/KEM.605.181.